Topics in Catalysis (2022) 65:595–603
https://doi.org/10.1007/s11244-021-01469-2

ORIGINAL PAPER

Voltammetric Determination of Ceftizoxime by a Carbon Paste Electrode Modified with Ionic Liquid and Cu $(Him)_2$ Nanoparticles

Somayeh Tajik[1] · Hadi Beitollahi[2] · Mahboobeh Shahsavari[3] · Iran Sheikhshoaie[3]

Accepted: 1 July 2021 / Published online: 20 July 2021

Abstract
Ceftizoxime (CFX) is used to reduce the infection caused by both gram-negative and gram-positive bacteria. In this report, a novel electrochemical sensor for CFX comprising a $Cu(Him)_2$ nanoparticles and ionic liquid (IL) hybride modified carbon paste electrode (CPE) has been developed. The structural properties of $Cu(Him)_2$ nanoparticles was characterized using energy-dispersive X-ray spectroscopy (EDX) analyses, X-ray diffraction (XRD), and field emission scanning electron microscopy (FESEM). The results illustrate that $Cu(Him)_2$/ILCPE exhibits an excellent electrocatalytic effect in the electrooxidation of CFX that leads to a considerable improvement in the corresponding anodic peak current. Under the best experimental conditions, the sensor exhibited a linear response to CFX from 2.0 to 1000.0 μM, with a limit of detection (LOD) of 0.5 nM. Finally, this also allows the development of a highly sensitive voltammetric sensor for the determination of CFX in pharmaceutical and biological samples.

Keywords Ceftizoxime · Cu $(Him)_2$ nanoparticles · Modified electrode · Carbon paste electrode

1 Introduction

Ceftizoxime (CFX) has been proposed as the third descendant cephalosporin antibiotic, which activates against aerobic of the gram-positive and -negative bacteria and declines putrefaction via interference in the wall by rupturing the wall and thus decays the bacteria [1, 2]. In fact, CFX has been introduced as one of the active agents against putrefaction with the extensive uses the treatment of susceptible infection like lung infections, skin and soft tissue, bone, and joint infections and other abdominal infection. Therefore, it is of special significance to quantitatively detect the analgesics and antibiotics in the biological fluids for the drug metabolisms [3, 4].

Researchers have presented numerous procedures like chromatography [5–7] and spectrophotometry [8, 9] to detect CFX. Nonetheless, such compounds consisting of sulfur cannot be efficiently detected by spectrophotometry due to the lack of light absorption of the compounds by them [10, 11]; hence, their derivatization would be developed. In other hand, the above techniques include difficult extraction phases for analyzing the real sample. Additionally, multiple materials must be consumed [12, 13]. For this reason, experts in the field must provide rapid sensitive analytical techniques.

Currently, researchers have largely employed electroanalytical procedures to the biomedical and pharmaceutical analyses as the biological reactions in humans and electrochemical reactions at the interface of the solution electrode undergo the same set of the electron transfer pathways. Electrochemical methods, due to their rapid response, simplicity, low cost, higher sensitivity, real-time detection, and acceptable selectivity with in-situ analysis are considerably studied in the pharmaceutical major compounds with the electrochemical activities [14–24].

Modification of the surfaces of such sensors with nanomaterials can enhance these advantages [25, 26].

As a result of easier fabrication process, compatibility with diverse kinds of modifier, as well as renewability, CPEs are

✉ Hadi Beitollahi
hadi_beitollahi@yahoo.com

[1] Research Center for Tropical and Infectious Diseases, Kerman University of Medical Sciences, Kerman, Iran

[2] Environment Department, Institute of Science and High Technology and Environmental Sciences, Graduate University of Advanced Technology, Kerman, Iran

[3] Department of Chemistry, Faculty of Science, Shahid Bahonar University of Kerman, 76175-133 Kerman, Iran

considerably employed as one of the proper matrices to prepare the modified electrodes. Additionally, the CPEs exhibit lower background currents than that of the noble metal electrodes or solid graphite [27–32].

Recently, nanomaterials have attracted increasing interest in different fields [33–36]. According to some studies, it is possible to design nanomaterials of the different types like single or hybrid/combinatorial nanostructures with distinct characteristics with the considerable differences from the common bulk materials. Nano-sized materials the extensive uses for preparing electrochemical sensors due their large surface areas, unique electronic, structural, mechanical and catalytic properties [37–39]. Hence, it would be of special significance to illustrate electronic and physicochemical interactions at the interface of the nano-material based electrodes with the intended analytes in order thoroughly apply the potential of the modern electro chemical sensors [40–48].

According to some studies, hybrid materials enjoy a combination of the organic and inorganic elements for generating a synergic effect of the greater functions of specific components that act by themselves. Moreover, researchers have largely considered the metal–organic hybrids as the modified-electrode substances because of their large surface areas, proper pore volumes, available cages, higher biocompatibility as well as uniform structures [49, 50].

The ligands consisting of imidazole have been considered to be poorer π-acceptors and more acceptable π –donors than that of the analogous pyridine consisting of the ligands acting as a reasonable acceptor because of the nearly low-lying π*-orbitals. Moreover, the deprotonation of the amino N–H proton may result in the perturbation of the electronic features of the metal complexes via establishing a metal–ligand interaction [51–54]. Because of the existence of the nitrogen donor atoms, imidazole may have coordination with diverse transition metal ions. In addition, researchers have introduced copper as one of the rich and more cost-effective transition metal elements on Earth and therefore copper-based catalyst has been greatly examined to design an inexpensive electro-catalyst [55–57].

Furthermore, deprotonation/protonation of imidazole moiety on the copper complexes can largely regulate electrochemical and redox features of the copper complexes [58–61]. Here, we proposes the construction of an electrochemical sensor to detect CFX by modification of a carbon paste electrode with $Cu(Him)_2$ and ionic liquid.

2 Experimental

2.1 Chemicals and Devices

Electrochemical properties were evaluated by Eco Chemie Autolab PGSTAT30 Potentiostat/Galvanostat System, the Netherlands. Then, we implemented a general purpose electrochemical system (GPES) software for monitoring the empirical conditions and applied conventional 3-electrodes cell at 25 ± 1 °C. Moreover, this research utilized the Ag/AgCl/KCl (3.0 M) electrode, the Cu $(Him)_2$/ILCPE as well as a platinum wire as the reference, working and auxiliary electrodes, respectively. Finally, we applied Metrohm 710 pH-meter to measure pHs.

Element analysis EDX was carried out by using the MIRA3 instrument. Examination of X-ray diffraction (XRD) patterns could be done through the use of XRD device model X'Pert Pro made in the Netherlands. Scanning electron microscope (FE-SEM, MIRA III, Czech Republic) was used to determine the morphology of composition $Cu(Him)_2$.

Purity common commercial products were the solvents and reagents employed in our research. Copper(II) sulfate, Imidazole (Him), Sodium bicarbonate ($NaHCO_3$), were bought from Sigma-Aldrich and each reagent was of analytical grade. All other reagents and ceftizoxime were Merck (Darmstadt, Germany) with analytical grade. In addition, orthophosphoric acid as well as the respective salts (KH_2PO_4, K_2HPO_4, and K_3PO4) with a pH ranging between 2.0 and 9.0 has been utilized to procure buffer solution (Table 1).

2.2 Preparation of Cu $(Him)_2$

The preparation of $Cu(Him)_2$ support was according to the literature. Briefly, a solution of Copper(II) sulfate (2.5 g, 10.1 mmol) into a 100 ml flask, Him (1.36 g, 20 mmol), and sodium bicarbonate (6.6 g, 78.56 mmol) were stirred for 3 h. The mixture is cooled to filter at environment temperature. The residue was washed with deionized water, to give the product as a blue powder. Then, we sealed autoclave and heated at 110 °C for 20 min.

2.3 Preparation of the Electrode

In this step, we mixed 10 mg of Cu $(Him)_2$ nanoparticles, 900 mg of graphite powder, as well as a certain content of ionic liquid and liquid paraffin for making Cu $(Him)_2$/ILCPE with a mortar and pestle. Afterwards, we poured the paste into the end of the glass tube (ca. 3.4 mm i.d. and 15 cm in length), and place a copper wire in paste for the electrical connection devices. Under certain circumstances, the excessive paste was pushed

Table 1 Structural specifications of $Cu(Him)_2$

Variable	Value
Molecular formula	$Cu(C_3H_3N_2)_2$
Molecular weight, g/mol	197.7
λ_{max}, nm	250

out of the tube and polished by a weighing paper for preparing a new surface.

In order to make comparisons, ionic liquid modified CPE (ILCPE) without Cu $(Him)_2$, Cu $(Him)_2$ carbon paste electrode (Cu $(Him)_2$/CPE) without ionic liquid and unmodified CPE in the absence of both ionic liquid and Cu $(Hin)_2$ NPs were similarly provided.

2.4 Procedure of Real Samples Preparation

CFX ampoule (with the labling 10 mg, Jaber Ebne Hayyan Pharmaceutical Company: Iran) was diluted with phosphate buffer solution (PBS) pH 5.0 and then, different amounts of the diluted solution was transferred into a 25 ml volumetric flask and diluted to the mark with the PBS at a pH of 5.0. Volume of CFX was analyzed by our procedure using the standard addition technique.

In the case of the urine samples, each sample was refrigerated shortly after collection. To perform the analyses, 10 ml of each sample was taken and centrifuged at 2000 rpm for a quarter, the supernatant was separated and filtered using a 0.45 µm filter paper. The solution was then transferred into and diluted to the mark in a 25 mL volumetric flask using PBS (pH = 5.0).Various amounts of SFX were spike into the samples for the purpose of analyses.

3 Results and Discussion

3.1 Characterization of Cu $(Him)_2$ Nanoparticles

3.1.1 EDX Analyses of Cu$(Him)_2$

The results of EDX show that all the elements; Cu, N and C in the sample are present. The weight percent of the elements Cu, N and C are 84.9, 9.11, 5.99 respectively. (Fig. 1 and Table 2).

3.2 Analysis of the X-Ray Powder Diffraction

XRD profiles of Cu$(Him)_2$ is shown in Fig. 2. The crystal phase is unique for Cu$(Him)_2$. This pattern shows which Cu$(Him)_2$ is pure crystalline phases without any impurities of the intermediates. As we have seen from the XRD pattern, this zeolite imidazole framework particle is well crystallized. This pattern shows the average size of particles about 15.6 nm.

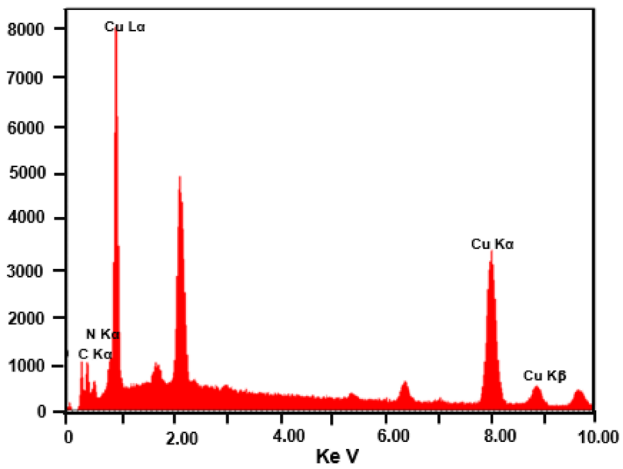

Fig. 1 EDX spectrum of Cu$(Him)_2$ particles

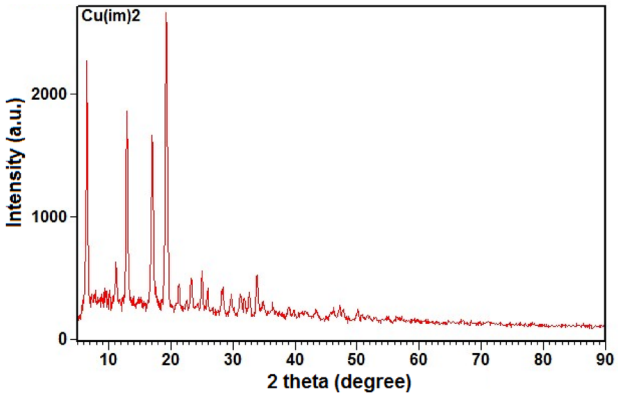

Fig. 2 Powder XRD pattern of the blue polymorph Cu$(Him)_2$

3.3 Sample Morphology

The surface morphologies of Cu$(Him)_2$ particles were studied by FESEM and are shown in Fig. 3. From these figures can be seen all particles have nanotube structure and also samples average size are about 74 and 90 nm.

Table 2 Quantitative results EDX spectrum of Cu$(Him)_2$ particles

Elt	Line	Int	Error	K	Kr	W%	A%	ZAF	Ox%	Pk/Bg	Class	LConf	HConf	Cat#
C	Ka	28.6	97.2235	0.0471	0.0428	5.99	20.08	0.7137	0	17.87	A	5.66	6.33	0
N	Ka	53.4	97.2235	0.0887	0.0805	9.11	26.16	0.8833	0	10.46	A	8.74	9.48	0
Cu	La	502.3	47.4222	0.8642	0.7842	84.9	53.76	0.9236	0	36.68	A	83.77	86.03	0
				1	0.9074	100	100		0					0

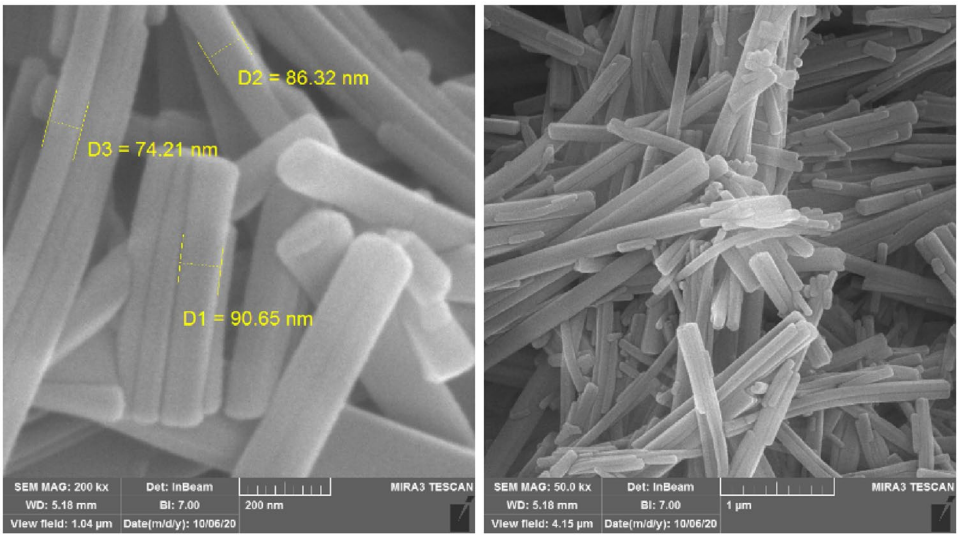

Fig. 3 FESEM images of the $Cu(Him)_2$

3.4 Electrochemical Profile of the CFX on the $Cu(Him)_2$ /ILCPE

Studies in the field have shown the dependence of the electro-chemical behaviour of CFX on the pH-value of the aqueous solutions. Hence, pH optimization would be of high importance for obtaining the electrocatalytic oxidation of CFX. It is notable that we examined the electrochemical behaviour of CFX in 0.1 M PBS at various pH-values ($2.0 < pH < 9.0$) at the $Cu(Him)_2$/ILCPE surface using CV. Furthermore, electro catalytic oxidation of CFX at the $Cu(Him)_2$/ILCPE surface was acceptable in acidic condition as compared to the basic or neutral media. From the highest current obtained in acidic conditions, pH 5.0 was selected as an optimized pH to electro catalyze CFX oxidation over $Cu(Him)_2$/ILCPE surface (Fig. 4). In addition, equal electron as well as proton contributed to the CFX electrochemical reaction at surface of $Cu(Him)_2$/ILCPE through the Ep slope vs. pH plot (Fig. 5).

Figure 6 represents the CV response for electrochemical oxidation of 500.0 nM CFX at the unmodified CPE (curve a), $Cu(Him)_2$/CPE (curve b), ILCPE (curve c) and $Cu(Him)_2$/ILCPE (curve d).

Figure 6 depicts the anodic peak potential of ~ 880 mV for CFX oxidation on the bare CPE surface (curve a) and 780 mV on the $Cu(Him)_2$/ILCPE surface (curve d). As seen in the curves, the peak potential CFX oxidation on the surface of the modified electrode switched from 100 mV to the negative values in comparison to the surface of the bare electrode. With regard to the CFX oxidation on the surface of $Cu(him)_2$/CPE (curve b) and $Cu(Him)_2$/ILCPE

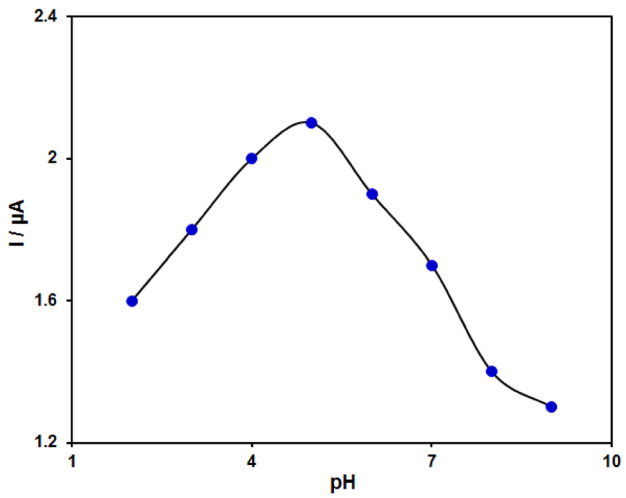

Fig. 4 Current-pH curve for electrooxidation of 100.0 nM CFX at the surface of $Cu(Him)_2$/ILCPE at various pH values (2.0–9.0) in 0.1 M phosphate buffered solution at a scan rate of 50 mV s^{-1}

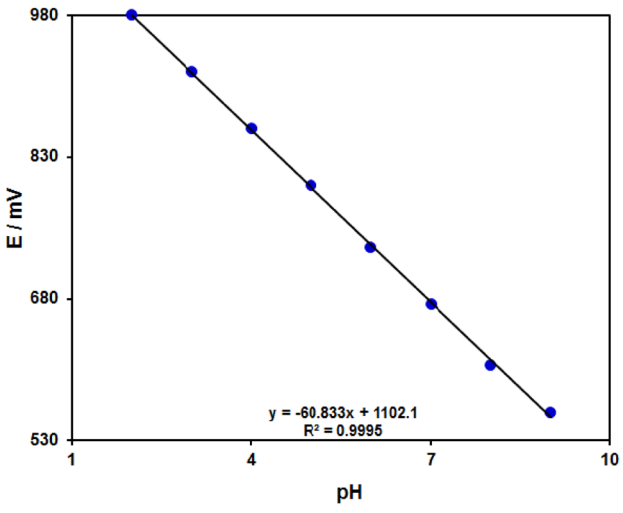

Fig. 5 E plot versus pH for electrooxidation of 100.0 nM CFX at the surface of $Cu(Him)_2$/ILCPE at various pH values (2.0–9.0) in 0.1 M phosphate buffered solution at a scan rate of 50 mV s^{-1}

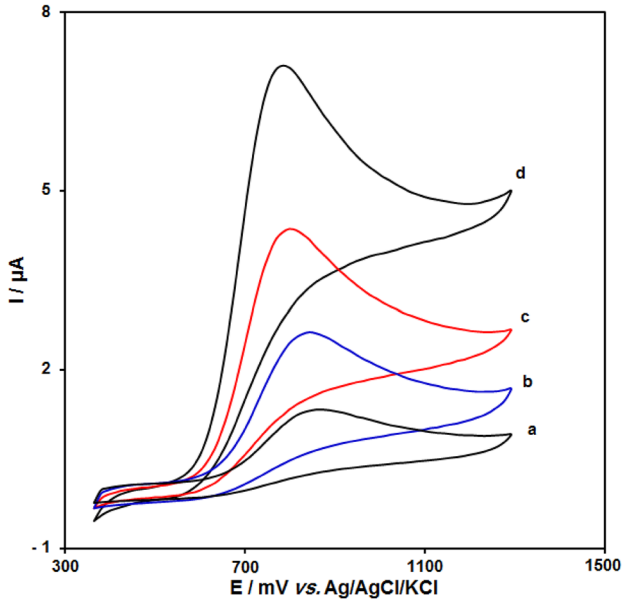

Fig. 6 CVs of bare CPE (**a**) $Cu(Him)_2$/CPE (**b**) ILCPE (**c**) and $Cu(Him)_2$/ILCPE (**d**) in exposure to CFX (500.0 nM) at the pH of 5.0 and the scan rate of 50 mV/s

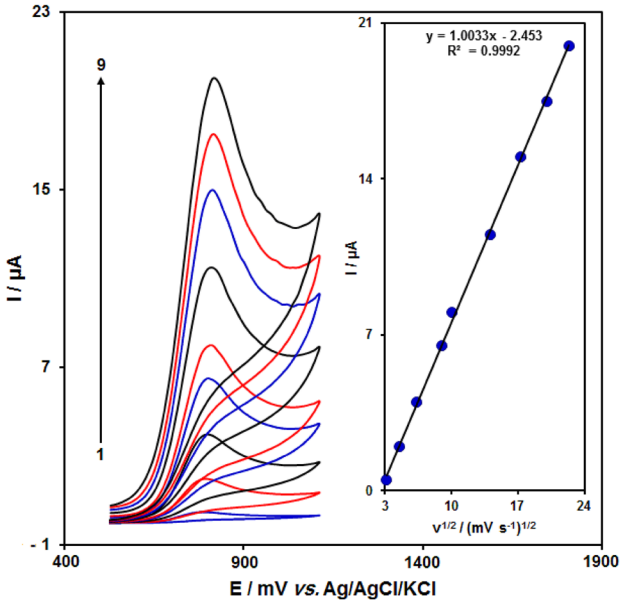

Fig. 7 CVs of $Cu(Him)_2$/ILCPE 0.1 M PBS (pH 5.0) containing 500.0 nM of CFX at various scan rates; 1–9 correspond to 10, 20, 40, 80, 100, 200, 300, 400 and 500 mV s^{-1}, respectively. Inset: variation of anodic peak current with square root of scan rate

(curve d), the anodic peak current enhanced on $Cu(Him)_2$/ILCPE compared to the $Cu(Him)_2$/CPE, which reveals the greater peak currents by ionic liquids (ILs) presence in the CPE. Researchers have shown several benefits for ILCPE like fast electron transfer, appropriate antifouling features, the catalytic nature of the ILs, as well as greater conductivity. Therefore, we put the IL mass into the paraffin oil and carbon which link the granules and observed that ILCPE conductivity significantly improved that matches our electrochemistry results. With regard to Fig. 6 (curves c & d), the oxidation peak current on the $Cu(Him)_2$/ILCPE surface is higher than that on the $Cu(Him)_2$/CPE surface. Moreover, we observed the $Cu(Him)_2$on IL surface on the electrochemical response, which is possibly caused by the probable features of $Cu(Him)_2$, such as the greater surface area, acceptable electrical conductivity and stronger chemical stability.

3.5 Effect of Scan Rate on the Results

In this step, we addressed the impacts of the rates of potential scan on the CFX oxidation current (Fig. 7) and showed the induced increase of the peak current via enhancing the potential scan rate. Moreover, we monitored diffusion in the oxidation processes, which was shown by linear dependence of the anodic peak current (Ip) on the square root of the potential scan rate ($\nu^{1/2}$).

Tafel-plot based on the outputs of the ascending section of the curve for current–voltage registered at the scan rate equal to 10 mVs^{-1} for CFX as depicted in Fig. 8. The mentioned section that is also called voltammogram referred to the Tafel area has been influenced through the kinetics of electron transfer between $Cu(Him)_2$/ILCPE and the substrate (CFX). Moreover, Tafel slopes of 0.1037 V was observed, showing the consistency with contribution of one electron at the rate determining step of the electrode procedure, assuming the charge transfer coefficient $\alpha = 0.43$.

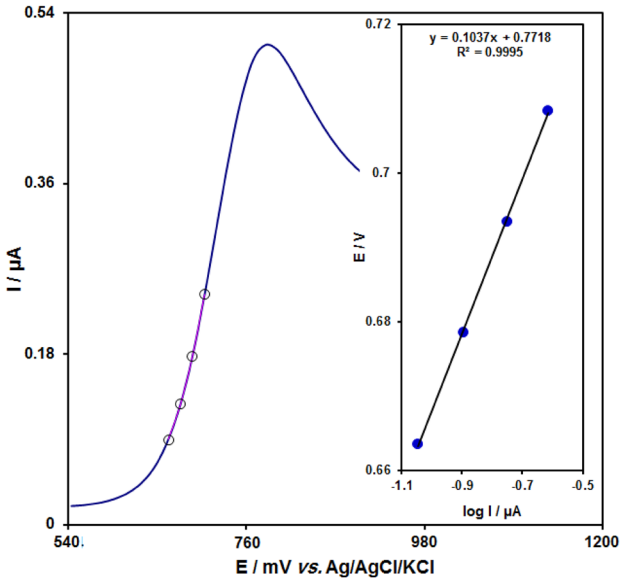

Fig. 8 LSV (at 10 mV s^{-1}) of a $Cu(Him)_2$/ILCPE in 0.1 M PBS at a pH 5.0 consisting of 500.0 nM CFX. These points represent outputs applied in Tafel plot and inset presents the Tafel plot obtained from LSV

3.6 Calibration Curve and LOD

It is possible to apply electro-oxidation peak currents of CFX at the surface of $Cu(Him)_2$/ILCPE for CFX detection in the solution. It is well-known that greater sensitivity and specific features for analytical uses have been proposed as the advantages of differential pulse voltammetry (DPV), we utilized $Cu(Him)_2$/ILCPE in 0.1 M PBS of various concentrations of CFX for DPV procedures (Fig. 9) (Step potential = 0.002 V, Modulation Amplitude = 0.02505 V). As seen in the figure, electro-catalytic peak current of the CFX oxidation at the surface of $Cu(Him)_2$/ILCPE has a linear dependence on the CFX concentration above ranges from 2.0 to 1000.0 µM (with a correlation coefficient of 0.9996) whereas LOD (3σ) equalled 0.5 nM. Table 3 presents a comparison of electrochemical techniques for the detection of CFX at the prepared electrode in this work and some other works.

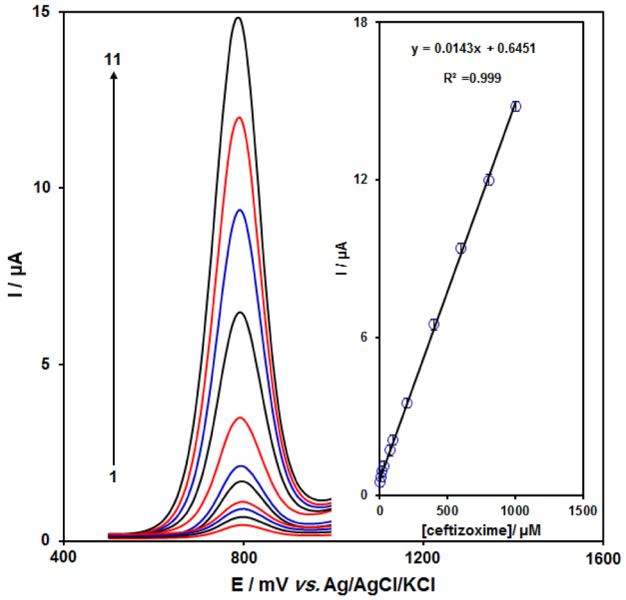

Fig. 9 DPVs of $Cu(Him)_2$/ILCPE in 0.1 M PBS (pH 5.0) consisting of various concentrations of CFX. 1–11 relative to 2.0, 7.5, 15.0, 30.0, 75.0, 100.0, 200.0, 400.0 600.0 and 800.0 and 1000.0 µM of CFX, respectively. The inset: the peak current plot as the function of CFX concentrations in ranges from 2.0–1000.0 µM

3.7 Real Sample Analysis

We applied this method to detect CFX in urine and CFX ampoule specimens for evaluating the utility of the modified electrode in the real samples. Moreover, we implemented the standard addition method. Table 4 reports the findings. As seen, CFX recoveries are reasonable and generalizability of the results has been shown with regard to the mean relative standard deviation (RSD).

4 Conclusion

The present research showed feasible quantification of the CFX concentration at the micromolar level by combining certain catalytic features of IL with the specific features of Cu $(Him)_2$ NPs like a greater surface area in a carbon paste environment. Cu $(Him)_2$/ILCPE sensor showed catalytic impact on the CFX oxidation via elevating its oxidation

Table 4 Ceftizoxime detection in real specimens via $Cu(Him)_2$/ILCPE. Each concentration is expressed in µM (n = 3)

Sample	Spiked	Found	Recovery (%)	R.S.D. (%)
Blood serum	0	3.0	–	3.5
	1.0	3.9	97.5	2.1
	2.0	5.2	104.0	1.9
	3.0	5.9	98.3	3.0
	4.0	7.1	101.4	2.4
Tablet	0	–	–	–
	5.0	4.9	98.0	2.9
	7.0	7.2	102.9	2.8
	9.0	8.8	97.8	1.7
	11.0	11.1	100.9	3.0

Table 3 A comparison of electrochemical techniques for the detection of CFX at the prepared electrode in this work and some other works

Electrochemical sensor	Method	Linear range	LOD	References
Hollow gold nanoparticles/reduced graphene oxide/pencil graphite electrode	Stripping differential pulse voltammetry	1×10^{-12}-1×10^{-9} M	3.5×10^{-13} M	[1]
Nano diamond-graphite nano mixture decorated with Ag nanoparticles/glassy carbon electrode	Linear sweep voltammetry	0.02–7 µM	6 nM	[4]
Poly(o-anisidine)/sodium dodesyl sulfate /Ni/carbon paste electrode	Linear sweep voltammetry	100–2000 µM	80 µM	[10]
Fullerene/glassy carbon electrode	Square-wave voltammetry	2.96–25.4 µM	0.00066 µM	[62]
$Cu(Him)_2$/ILCPE	DPV	2.0–1000.0 µM	0.5 nM	This work

peak. The linear current response to CFX concentration was obtained to be from 2.0 to 1000.0 μM with a detection limit of 0.5 nM and a sensitivity of 0.0143 μA μM^{-1}. Hence, researchers have designed a more sensitive electro-chemical technique to detect CFX in pharmaceutical and clinical samples. Such an electrode would offer specific advantages over the common electrodes due to easier construction processes, very good catalytic activities, simplicity as well as sensitivity. Hence, $Cu(Him)_2$/ILCPE has shown to be highly promising for potential sensing utilizations.

References

1. Azadmehr F, Zarei K (2020) Ultrasensitive determination of ceftizoxime using pencil graphite electrode modified by hollow gold nanoparticles/reduced graphene oxide. Arab J Chem 13:1890–1900
2. Beytur M, Kardaş F, Akyıldırım O, Özkan A, Bankoğlu B, Yüksek H, Atar N (2018) A highly selective and sensitive voltammetric sensor with molecularly imprinted polymer based silver@gold nanoparticles/ionic liquid modified glassy carbon electrode for determination of ceftizoxime. J Mol Liq 251:212–217
3. Wang L, Zheng X, Zhong W, Chen J, Jiang J, Hu P (2016) Validation and application of an LC–MS–MS method for the determination of ceftizoxime in human serum and urine. J Chromatogram Sci 54:713–719
4. Shahrokhian S, Ranjbar S, Ghalkhani M (2016) Modification of the electrode surface by Ag nanoparticles decorated nano diamond-graphite for voltammetric determination of ceftizoxime. Electroanalysis 28:469–476
5. Suzuki A, Noda K, Noguchi H (1980) High-performance liquid chromatographic determination of ceftizoxime, a new cephalosporin antibiotic, in rat serum, bile and urine. J Chromatogr B 182:448–453
6. Sanli S, Sanli N, Gumustas M, Ozkan SA, Karadas N, Aboul-Enein HY (2011) Simultaneous estimation of ceftazidime and ceftizoxime in pharmaceutical formulations by HPLC method. Chromatographia 74:549
7. Mccormick EM, Echols RM, Rosano TG (1984) Liquid chromatographic assay of ceftizoxime in sera of normal and uremic patients. Antimicrob Agents Chemother 25:336–338
8. Al-Momani IF (2001) Spectrophotometric determination of selected cephalosporins in drug formulations using flow injection analysis. J Pharma Biomed Anal 25:751–757
9. El Walily AFM, Gazy AAK, Belal SF, Khamis EF (2000) Use of cerium (IV) in the spectrophotometric and spectrofluorimetric determinations of penicillins and cephalosporins in their pharmaceutical preparations. Spectros Lett 33:931–948
10. Ojani R, Raoof JB, Zamani S (2010) A novel sensor for cephalosporins based on electrocatalytic oxidation by poly (o-anisidine)/SDS/Ni modified carbon paste electrode. Talanta 81:1522–1528
11. Owens GS, Lacourse WR (1996) Pulsed electrochemical detection of sulfur-containing compounds following microbore liquid chromatography. Curr Sep 14:82–89
12. Yola ML, Göde C, Atar N (2017) Molecular imprinting polymer with polyoxometalate/carbon nitride nanotubes for electrochemical recognition of bilirubin. Electrochim Acta 246:135–140
13. Kardaş F, Beytur M, Akyıldırım O, Yüksek H, Yola ML, Atar N (2017) Electrochemical detection of atrazine in wastewater samples by copper oxide (CuO) nanoparticles ionic liquid modified electrode. J Mol Liq 248:360–363
14. Srivastava AK, Upadhyay SS, Rawool CR, Punde NS, Rajpurohit AS (2019) Voltammetric techniques for the analysis of drugs using nanomaterials based chemically modified electrodes. Curr Anall Chem 15:249–276
15. Tajik S, Beitollahi H, Garkani Nejad F, Sheikhshoaie I, Sugih Nugraha A, Won Jang H, Yamauchi Y, Shokouhimehr M (2021) Performance of metal–organic frameworks in the electrochemical sensing of environmental pollutants. J Mater Chem A 9:8195–8220
16. Srikanta S, Parmeswara Naik P, Krishanamurthy G (2019) Electrochemical behaviour of 5-methoxy-5,6-bis(3-nitropheyl-4,5-dihydro-1,2,4-triazine-3(2H))-thione in presence of salicylaldehyde on zinc cathode with surface morphology and biological activity. Asian J Green Chem 4:149–158
17. Siddeeg SM, Alsaiari NS, Tahoon MA, Rebah FB (2020) The application of nanomaterials as electrode modifiers for the electrochemical detection of ascorbic acid. Int J Electrochem Sci 15:3327–3346
18. Elobeid WH, Elbashir AA (2019) Development of chemically modified pencil graphite electrode based on benzo-18-crown-6 and multi-walled CNTs for determination of lead in water samples. Prog Chem Biochem Res 2:24–33
19. Rshad S, Mofidi Rasi R (2019) Electrocatalytic oxidation of sulfite Ion at the surface carbon ceramic modified electrode with prussian blue. Eurasian Chem Commun 1:43–52
20. Nejad FG, Tajik S, Beitollahi H, Sheikhshoaie I (2021) Magnetic nanomaterials based electrochemical (bio) sensors for food analysis. Talanta 228:122075
21. Taei M, Salavati H, Fouladgar M, Abbaszadeha E (2020) Simultaneous determination of sunset yellow and tartrazine in soft drinks samples using nanocrystallites of spinel ferrite-modified electrode. Quarte J Iran Chem Commun 8:67–79
22. Rabiee N, Safarkhani M, Rabiee M (2018) Ultra-sensitive electrochemical on-line determination of Clarithromycin based on Poly (L-Aspartic acid)/graphite oxide/pristine graphene/glassy carbon electrode. Asian J Nanosci Mater 1:63–73
23. Tajik S, Beitollahi H, Asl MS, Jang HW, Shokouhimehr M (2021) BN-Fe_3O_4-Pd nanocomposite modified carbon paste electrode: Efficient voltammetric sensor for sulfamethoxazole. Ceram Int 47:13903–13911
24. Al-Jawadi AM, Majeed MI (2021) Detection of anticancer drug by electrochemical sensors at modified electrode (MWCNT/polyEosin-Y). Nanomed Res J 6:50–59
25. Messaoud NB, Ghica ME, Dridi C, Ali MB, Brett CM (2017) Electrochemical sensor based on multiwalled carbon nanotube and gold nanoparticle modified electrode for the sensitive detection of bisphenol A. Sens Actuators B Chem 253:513–522
26. Khalilzadeh MA, Tajik S, Beitollahi H, Venditti RA (2020) Green synthesis of magnetic nanocomposite with iron oxide deposited on cellulose nanocrystals with copper (Fe_3O_4@ CNC/Cu): investigation of catalytic activity for the development of a venlafaxine electrochemical sensor. Indust Eng Chem Res 59:4219–4228
27. Batista LCD, Santos TIS, Santos JEL, da Silva DR, Martínez-Huitle C (2021) Metal organic Framework-235 (MOF-235) modified carbon paste electrode for catechol determination in water. Electroanalysis 33:57–65
28. Payehghadr M, Taherkhani Y, Maleki A, Nourifard F (2020) Selective and sensitive voltammetric sensor for methocarbamol determination by molecularly imprinted polymer modified carbon paste electrode. Eurasian Chem Commun 2:982–990
29. Kalcher K, Kauffmann JM, Wang J, Švancara I, Vytřas K, Neuhold C, Yang Z (1995) Sensors based on carbon paste in electrochemical analysis: a review with particular emphasis on the period 1990–1993. Electroanalysis 7:5–22

30. Mahmoud AM, Mahnashi MH, El-Wekil MM (2021) Indirect differential pulse voltammetric analysis of cyanide at porous copper based metal organic framework modified carbon paste electrode: application to different water samples. Talanta 221:121562
31. Abrishamkar M, Ehsani Tilami S, Hosseini Kaldozakh S (2020) Electrocatalytic oxidation of cefixime at the surface of modified carbon paste electrode with synthesized nano zeolite. Adv J Chem A 3:767–776
32. Payehghadr M, Adineh Salarvand S, Nourifard F, Rofouei MK, Bahramipanah N (2019) Construction of modified carbon paste electrode by a new pantazene ligand for ultra-trace determination of ion silver in real samples. Adv J Chem Section A 2:377–385
33. Akça A, Karaman O, Karaman C (2021) Mechanistic insights into catalytic reduction of N_2O by CO over Cu-embedded graphene: a density functional theory perspective. ECS J Solid State Sci Technol 10:041003
34. Karimi-Maleh H, Bananezhad A, Ganjali MR, Norouzi P, Sadrnia A (2018) Surface amplification of pencil graphite electrode with polypyrrole and reduced graphene oxide for fabrication of a guanine/adenine DNA based electrochemical biosensors for determination of didanosine anticancer drug. Appl Surf Sci 441:55–60
35. Karaman C (2021) Orange peel derived-nitrogen and sulfur Co-doped carbon dots: a nano-booster for enhancing ORR electrocatalytic performance of 3D graphene networks. Electroanalysis 33:1356–1369
36. Karaman C, Karaman O, Atar N, Yola ML (2021) Electrochemical immunosensor development based on core-shell high-crystalline graphitic carbon nitride@carbon dots and Cd0.5Zn0.5S/d-Ti_3C_2Tx MXene composite for heart-type fatty acid–binding protein detection. Microchim Acta 188:1–15
37. Tahernejad-Javazmi F, Shabani-Nooshabadi M, Karimi-Maleh H (2019) 3D reduced graphene oxide/$FeNi_3$-ionic liquid nanocomposite modified sensor; an electrical synergic effect for development of tert-butylhydroquinone and folic acid sensor. Compos Part B 172:666–670
38. Tajik S, Beitollahi H, Jang HW, Shokouhimehr M (2021) A screen printed electrode modified with Fe_3O_4@polypyrrole-Pt core-shell nanoparticles for electrochemical detection of 6-mercaptopurine and 6-thioguanine. Talanta 232:122379
39. Shaikh UU, Tamboli Q, Pathange SM, Dahan ZA, Pudukulathan Z (2018) An efficient method for chemoselective acetylation of activated alcohols using nano $ZnFe_2O_4$ as catalyst. Chem Methodol 2:73–82
40. Shahzad H, Ahmadi R, Sheshmani S (2020) Investigating the performance of nano structure C60 as nano-carriers of anticancer cytarabine, a DFT study. Asian J Green Chem 4:355–366
41. Du H, Xie Y, Wang J (2021) Nanomaterial-sensors for herbicides detection using electrochemical techniques and prospect applications. TrAC Trends Anal Chem 116178.
42. Khataee A, Sohrabi H, Arbabzadeh O, Khaaki P, Majidi MR (2021) Frontiers in conventional and nanomaterials based electrochemical sensing and biosensing approaches for Ochratoxin A analysis in foodstuffs: a review. Food Chem Toxicol 112030.
43. Sheikhshoaie I, Rezazadeh A, Ramezanpour S (2018) Removal of Pb (II) from aqueous solution by gel combustion of a new nano sized Co_3O_4/ZnO composite. Asian J Nanosci Mater 1:271–281
44. Madadi Z, Soltanieh M, Bagheri Lotfabad T, Nazari S (2019) Green synthesis of titanium dioxide nanoparticles with Glycyrrhiza glabra and their photocatalytic activity. Asian J Green Chem 4:256–268
45. Ghafour Taher S, Abdulkareem Omar K, Mohammed Faqi-Ahmed B (2019) Green and selective oxidation of alcohols using MnO_2 nanoparticles under solvent-free condition using microwave irradiation. Asian J Green Chem 4:231–238
46. Fazal-ur-Rehman M, Qayyum I (2020) Biomedical scope of gold nanoparticles in medical sciences; an advancement in cancer therapy. J Med Chem Sci 3:399–407
47. Maleh HK, Orooji Y, Karimi F, Alizadeh M, Baghayeri M, Rouhi J, Tajik S, Beitollahi H, Agarwal S, Gupta VK, Rajendran S, Ayati A, Fu L, Sanati A, Tanhaei B, Sen F, Shabani-nooshabadi M, Asrami PN, Al-Othman A (2021) A critical review on the use of potentiometric based biosensors for biomarkers detection. Biosens Bioelectron 184:113252
48. Karimi-Maleh H, Alizadeh M, Orooji Y, Karimi F, Baghayeri M, Rouhi J, Tajik S, Beitollahi H, Agarwal S, Gupta VK, Rajendran S, Rostamnia S, Fu L, Saberi-Movahed F, Samira M (2021) Guanine-based DNA biosensor amplified with Pt/SWCNTs nanocomposite as analytical tool for nanomolar determination of daunorubicin as an anticancer drug: a docking/experimental investigation. Ind Eng Chem Res 60:816–823
49. Zhou K, Shen D, Li X, Chen Y, Hou L, Zhang Y, Sha J (2020) Molybdenum oxide-based metal-organic framework/polypyrrole nanocomposites for enhancing electrochemical detection of dopamine. Talanta 209:120507
50. Dong Y, Yang L, Zhang L (2017) Simultaneous electrochemical detection of benzimidazole fungicides carbendazim and thiabendazole using a novel nanohybrid material-modified electrode. J Agric Food Chem 65:727–736
51. Haga MA, Kobayashi K, Terada K (2007) Fabrication and functions of surface nanomaterials based on multilayered or nanoarrayed assembly of metal complexes. Coord Chem Rev 251(21–24):2688–2701
52. Su CC, Jan HC, Kuo-Yih H, Shyh-Jiun L, Shion-Wen W, Sue-Lein W, Sheng-Nan L (1992) Bonding properties of Cu (II)-imidazole chromophores: spectroscopic and electrochemical properties of monosubstituted imidazole copper (II) complexes. Molecular structure of [Cu (4-methylimidazole)$_4$ (ClO_4) $_2$]. Inorg Chim Acta 196:231–240
53. Kumar P, Joseph A, Ramamurthy PC, Subramanian S (2012) Lead ion sensor with electrodes modified by imidazole-functionalized polyaniline. Microchim Acta 177:317–323
54. Zhang SS, Niu SY, Qu B, Jie GF, Xu H, Ding CF (2005) Studies on the interaction mechanism between hexakis (imidazole) manganese (II) terephthalate and DNA and preparation of DNA electrochemical sensor. J Inorg Biochem 99:2340–2347
55. Zhao Z, Zhou B, Su Z, Ma H, Li C (2008) A new [As3Mo3O15] 3− fragment decorated with Cu (I)-imi (imi= imidazole) complexes: Synthesis, structure and electrochemical properties. Inorg Chem Commun 11:648–651
56. Oberhausen KJ, O'brien RJ, Richardson JF, Buchanan RM (1990) New tripodal Cu (II) complexes containing imidazole ligands. Inorg Chim Acta 173:145–154
57. Wei X, Li N, Zhang X (2017) Cu@ C nanoporous composites containing little copper oxides derived from dimethyl imidazole modified MOF199 as electrocatalysts for hydrogen evolution reaction. Appl Surf Sci 425:663–673
58. Forster RJ, Pellegrin Y, Keyes TE (2007) pH effects on the rate of heterogeneous electron transfer across a fluorine doped tin oxide/monolayer interface. Electrochem Commun 9:1899–1906
59. Liu F, Wang K, Bai G, Zhang Y, Gao L (2004) The pH-induced emission switching and interesting DNA-binding properties of a novel dinuclear ruthenium (II) complex. Inorg Chem 43:1799–1806
60. Barman K, Jasimuddin S (2014) Electrochemical detection of adenine and guanine using a self-assembled copper (II)–thiophenyl-azo-imidazole complex monolayer modified gold electrode. RSC Adv 4:49819–49826

61. Neelakantan MA, Sundaram M, Sivasankaran Nair M (2011) Solution equilibria of Ni (II), Cu (II), and Zn (II) complexes involving pyridoxine and imidazole containing ligands: pH metric, spectral, electrochemical, and biological studies. J Chem Eng Data 56:2527–2535
62. Jain R, Rather JA, Dwivedi A (2010) Highly sensitive and selective voltammetric sensor fullerene modified glassy carbon electrode for determination of cefitizoxime in solubilized system. Electroanalysis 22:2600–2606